Available online at www.sciencedirect.com
SCIENCE DIRECT®
Biochemical and Biophysical Research Communications 324 (2004) 154–165
BBRC
www.elsevier.com/locate/ybbrc

Gangliosides of organ-confined versus metastatic androgen-receptor-negative prostate cancer

Mepur H. Ravindranath[a,*], Sakunthala Muthugounder[a], Naftali Presser[a], Senthamil R. Selvan[b], Jacques Portoukalian[c], Stanley Brosman[d], Donald L. Morton[a]

[a] *Laboratory of Glycoimmunotherapy, John Wayne Cancer Institute, 2200 Santa Monica Blvd., Santa Monica, CA 90404-2302, United States*
[b] *Cell Biology Laboratory, Hoag Cancer Center, Newport Beach, CA 92663, United States*
[c] *INSERM U.346, Hospital Edouard-Herriot, 69437 Lyon Cx 03, France*
[d] *Pacific Clinical Research, 2021 Santa Monica Blvd., Santa Monica, CA 90404, United States*

Received 16 August 2004

Abstract

Prior development of a unique androgen-receptor (AR)-negative cell line (HH870) from organ-confined (T2b) human prostate cancer (CaP) enabled comparison of the gangliosides associated with normal and neoplastic prostate epithelial cells, organ-confined versus metastatic (DU 145, PC-3), and AR-negative versus AR-positive CaP cell lines. Resorcinol–HCl and specific monoclonal antibodies were used to characterize gangliosides on 2D-chromatograms, and to visualize them on the cell surface with confocal-fluorescence microscopy. AR-negative cells expressed GM1b, GM2, GD2, GD1a, and GM3. GM1a, GD1b, and GT1b were undetectable. GM1b and GD1a were more prominent in AR-negative than in AR-positive cells. PC-3 and HH870 cells were unique in the expression of *O*-acetylGD2 (*O*-AcGD2) and two α2,3-sialidase-resistant, alkali-susceptible GMR17-reactive gangliosides. Expression of GD1a, GM1b, doublets of GD3, GD2, and *O*-AcGD2, and the presence of an additional alkali-labile-14.G2a-reactive ganglioside, two alkali-susceptible, and three alkali-resistant GMR17-reactive gangliosides makes HH870 a potential component of a polyvalent-vaccine for active-specific immunotherapy of CaP.

Keywords: Gangliosides; Prostate cancer; Androgen-receptor; Organ-confined; Metastasis; *O*-AcetylGD2; 2D-chromatogram; HPLC; Confocal-fluorescence-microscopy

Gangliosides are a unique class of glycoantigens implicated in tumor progression, proliferation, invasion, angiogenesis, and immunosuppression [1–9]. These amphophilic molecules have a hydrophilic head group (sialic acids, lactose) and a hydrophobic tail group (sphingosine and a long-chain fatty acid) [10]. Gangliosides are overexpressed on the tumor cell surface; these T-cell independent antigens [11] may serve as targets for passive [12] and active-specific [13,14] immunotherapy. The nature and distribution of gangliosides differ between normal and neoplastic cells, and among specific cancers [15].

Although GM3, GM2, GD3, and GD2 have been identified in human prostate cancer (CaP) tissue [16–18], the ganglioside profile of established human CaP cell lines is not known. Of the four American Type Culture Collection (ATCC) cell lines, two (LNCaP FGC and LNCaP FGC-10) are androgen-receptor (AR)-positive (+) cells from lymph node metastases, and two (DU 145 and PC-3) are AR-negative (−) cells from brain and bone metastases. Recently, Selvan et al. [19] have developed an AR (−) cell line (HH870) from an organ-confined CaP (stage T2b). This cell line provides an opportunity to compare the ganglioside signatures of

* Corresponding author. Fax: +1 310 449 5259.
E-mail address: Ravindranathm@jwci.org (M.H. Ravindranath).

0006-291X/$ - see front matter © 2004 Elsevier Inc. All rights reserved.
doi:10.1016/j.bbrc.2004.09.029

CaP cell lines derived from organ-confined versus metastasized AR-negative CaP.

This investigation used monoclonal antibodies (MAbs), resorcinol staining, and mobility assessment to characterize the ganglioside signatures of human CaP cell lines. Our objective was to identify a cell line with optimal expression of major CaP gangliosides for active-specific immunotherapy of CaP.

Materials and methods

Prostate cancer cell lines. Three AR (−) CaP cell lines were used in this study: PC-3 (ATCC, CRL-1435) was initiated from a bone metastasis, DU 145 (ATCC, HTB-81) was isolated from a brain lesion, and HH870 (Hoag Cancer Center, Newport Beach, CA) was developed from an organ-confined primary tumor that had been resected from the right mid-gland and apex of the prostate in a 56-year old, previously untreated white male. This tumor was Gleason grade 3/4, with no evidence of vascular or perineural invasion or extracapsular extension (stage T2b). At the time of surgery, the patient had a serum prostate-specific antigen level of 5.65 ng/ml. Bone scans and chest X-rays revealed no metastatic disease. Androgen receptor was not detectable in the cell line by immunocytochemistry or by Western blot analysis [19].

Two CaP cell lines that expressed receptors for 5-α-dihydrotestosterone were used as AR (+) lines: LNCaP clones FGC (ATCC, CRL-1740) and FGC-10 (ATCC, CRL-10995). Normal prostate epithelial cells (PrEC) were obtained from Cambrex (BioScience Walkersville, MD) and cultured in their respective growth media (PrEGM, CC-4177, Cambrex). Murine YAC-1 lymphoma cell line (ATCC No: TIB-160) was used to isolate GM1b.

Cells were grown in RPMI medium 1640 with glutamine (Invitrogen, Carlsbad, CA) supplemented with 10% fetal calf serum, Hepes buffer, gentamicin (5 mg %), and fungizone (0.5 mg %), at 37 °C in a humidified atmosphere (95% air/5% CO_2). The cells were detached with sterile EDTA-dextrose (137 mM sodium chloride, 5.4 mM potassium chloride, 5.6 mM dextrose, 0.54 mM ethylenediaminetetraacetate (EDTA), and 7.1 mM sodium bicarbonate) at 37 °C for 5 min, recovered with cold RPMI 1640-human serum albumin (4%; HSA, Gropo Grifols de America, Miami, FL), and resuspended in the same medium. Harvested cells were cryopreserved in RPMI-7.5% HSA containing 10% dimethyl sulfoxide (DMSO) and stored under liquid nitrogen. When required, the cryopreserved cells were half-thawed at 37 °C in a water bath for 15–30 s and further thawed at room temperature. The cell suspension was washed with RPMI-4% HSA, centrifuged, and resuspended in the same medium. Cell count was measured using a hemocytometer and viability by trypan blue (0.2%) dye exclusion method.

Glycolipid extraction from cell pellets. Glycolipids were extracted following a protocol described earlier [20]. Freshly harvested or cyropreserved cells resuspended in RPMI-4% HSA were counted and rewashed in PBS. Methanol (M) was added to the pellets (v/v, 1/10), vortexed, mixed with equal volume of chloroform, and allowed to stand at room temperature for 5 h. After centrifugation, the supernatant was separated and evaporated to dryness under nitrogen. The dried moiety was resuspended in 2 ml chloroform/methanol (v/v, 2/1). After the suspension was centrifuged, the supernatant was collected, dried over nitrogen, and redissolved in 4 ml chloroform/methanol (v/v, 1/1). The final ratio of the suspension was adjusted to chloroform/methanol/PBS (v/v/v, 1/1/0.7). The extract was centrifuged; the upper phase containing gangliosides was recovered and the lower phase was re-extracted with methanol/PBS. The upper phase was recovered thrice and pooled.

Isolation of gangliosides. Gangliosides were isolated on columns (ENVI-Chrom P, Supelco, Bellefonte, PA) containing a resin made of small, non-ionic, highly cross-linked styrene-divinylbenzene beads [21]. The columns were fixed in Visiprep solid phase extraction vacuum manifold (Supelco). Initially the column was conditioned by adding methanol followed by PBS. The upper phase containing gangliosides was layered on the column, the flow rate was adjusted in drops, and the solution was collected. The column was washed with distilled water twice in order to remove non-lipid contaminants such as salts, sugars, and amino acids. Water was removed completely. Gangliosides were eluted from the column by adding 3 ml methanol and then 3 ml chloroform:methanol (C:M) (v/v, 2/1). Eluent was dried over nitrogen and the gangliosides were dissolved in chloroform/methanol (v/v, 2/1) and stored at −20 °C.

High-performance thin-layer chromatography. Ganglioside signatures of CaP cells were analyzed by high-performance thin-layer chromatography (HPTLC) as described earlier [20]. HPTLC plates (10 × 10 cm) precoated with Silica Gel 60 (glass or aluminium backing) (E. Merck, Darmstadt, Germany) were used. Two-dimensional HPTLC was performed using two different solvent systems. The sample was separated in the first dimension in chloroform/methanol/0.2% $CaCl_2$ (v/v/v, 55/45/10,). Solvent systems were equilibrated several hours before use in TLC chamber. The plate was dried in a vacuum desiccator overnight and run in the second dimension in chloroform/methanol/2.5 M NH_4OH in 0.25% KCl (v/v/v, 50/40/10).

The following gangliosides were screened for purity and homogeneity: GM3 (Sigma: G 5642), GM2 (Sigma: G 8397), *N*-glycol-GM3 (Gift from Dr. Adriana Carr, Center for Molecular Immunology, Habana, Cuba), GM1a (Sigma: G 7641), GD3 (Calbiochem: 345752), GD1a (Sigma: G 2392), GD2 (Advanced Immunochem, Long Beach, IG6), GD1b (Sigma: G 8146), and GT1b (Sigma: G 3767). These gangliosides were used as reference standards for TLC and as antigens for ELISA. The gangliosides were spotted onto the plates using Linomat (CAMAG Scientific, Wilmington, NC). The plates were pre-run in chloroform to eliminate neutral lipid and other contaminants that may interfere with the mobility of gangliosides. Gangliosides were visualized by heating at 100 °C after spraying with resorcinol–HCl reagent (10 ml of 2% resorcinol in water, 40 ml concentrated HCl, and 0.125 ml of 0.1 M copper sulfate). Each chromatogram represented ganglioside extract from 25×10^6 cells.

Specificity of monoclonal antibodies and immunostaining. Gangliosides were separated on aluminium-backed silica gel plates, and the plates were dipped in 0.2% solution of polyisobutyl-methacrylate in hexane for 1 min. After drying, plates were blocked with PBS–1% HSA for 30 min, washed with PBS, and dried. Immunostaining was performed with antiganglioside murine monoclonal antibodies (MAbs) [22,23] (Fig. 1A) whose specificity had been tested with an ELISA protocol described elsewhere [24]. Each plate was overlaid with a MAb diluted in PBS-1% HSA for 2 h at 37 °C. The dilution used for immunostaining and the protein concentration of the primary antibodies used for ELISA are as follows: GMB16 (anti-GM1a; 1/400 for immunostaining; 200 ng/well for ELISA); KM696 (anti-GM2; I/1000, 500 ng/well); 14.G2a (anti-GD2; 1/250, 250 ng/well); MB3.6 (anti-GD3; 1/250, 250 ng/well); GGR12 (anti-GD1b; 1/200, 1 μg/well); 14F7 (1/1000, 40 ng/well); GD1a-1 (1/500, 250 ng/well); GMR17 (anti-GD1a/GM1b; 1/800, 200 ng/well); GMR5 (anti-GT1b; 1/500, 200 ng/well); and GMR11 (anti-GT1a; 1/400). The plates were then washed with PBS (for 3 min) thrice, dried, and incubated with biotinylated rabbit anti-mouse IgG (Jackson Immunoresearch, West Grove, PA; 315-065-008) or rabbit anti-mouse IgM (315-065-049) diluted at 1/500 for 1 h at 37 °C. The plates were washed thrice in PBS, dried, and incubated for 45 min in streptavidin-peroxidase (Jackson Immunoresearch; 016-030-084) diluted in PBS at 1/2500. The plates were developed with 4-chloro-1-naphthol solution (10 ml) and H_2O_2 (5 μl).

Immunostaining with GMR17 after sialidase treatment. Gangliosides isolated from PC-3 cell lines were treated with 50 mU of α2,3-

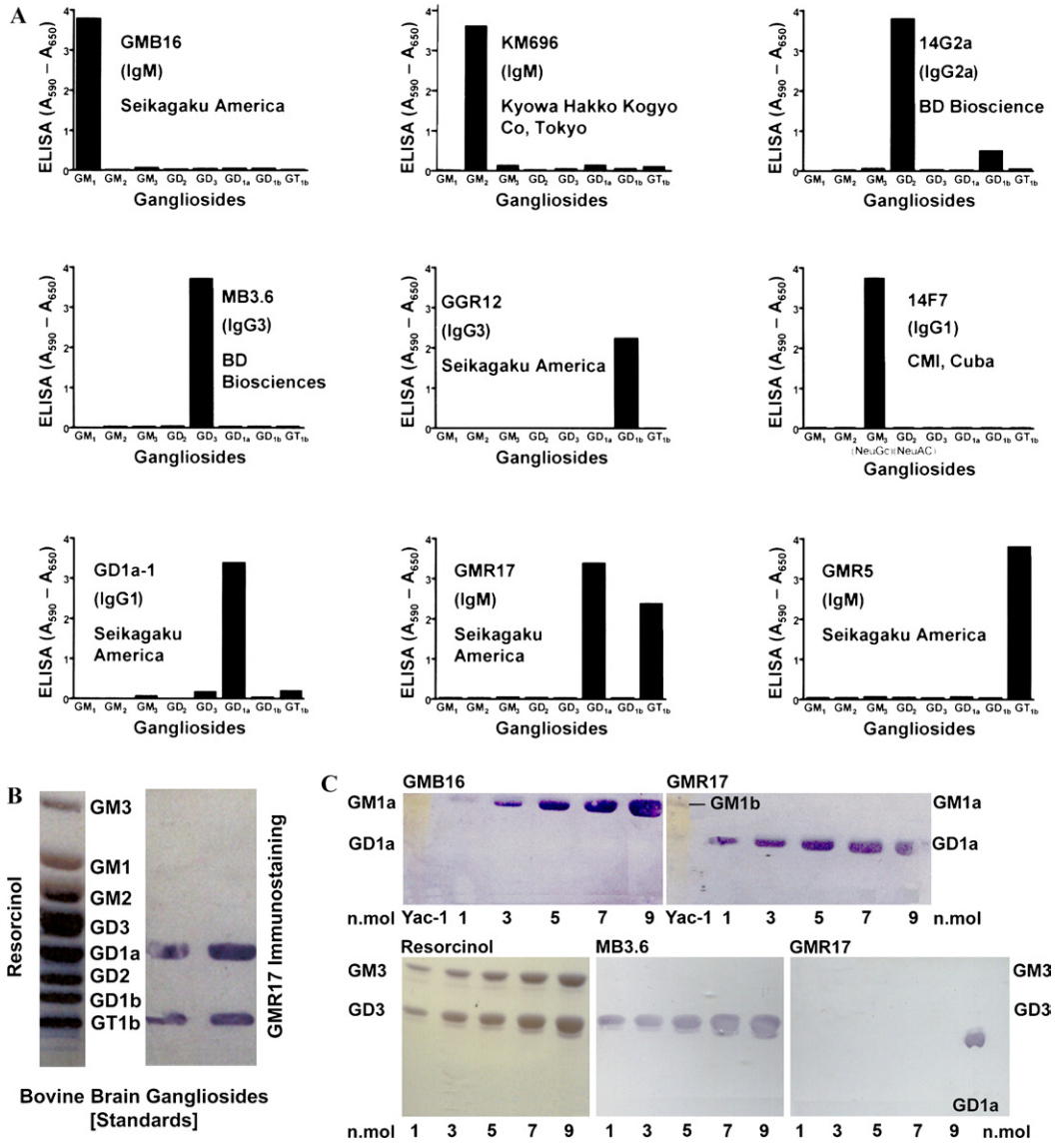

Fig. 1. Specificity of antiganglioside murine monoclonal antibodies. (A) All monoclonal antibodies except 14F7 are commercially available. The clones used include GMB16 (anti-GM1), KM696 (anti-GM2), 14.G2a (anti-GD2), MB3.6 (anti-GD3), GGR12 (anti-GD1b), 14F7 (anti-GM3-NeuGc), GD1a-1 (anti-GD1a), GMR17 (anti-GD1a), and GMR5 (anti-GT1b). All monoclonal antibodies except GMR17 showed remarkable specificity for their respective target antigens. Eight gangliosides (purified to >98%) were coated onto microtiter plates (3 nmol/well). Antibody titers were measured in ELISA microtiter plate reader at 490 nm, absorption maxima (λ) of quinone formed in the presence of OPDE/H_2O_2 and 6N sulfuric acid, and at 650 nm, for background correction. (B) Immunostaining of standard gangliosides with GMR17. Resorcinol profile is given for comparison. Although all the gangliosides were present, GMR17 immunostained only GD1a and GT1b. This observation confirms that GMR17 is not specific for GD1a but it recognizes the GD1a epitope on GT1b. (C) Immunostaining of one-dimensional thin-layer chromatograms with GMB16 (anti-GM1), GMR17 (anti-GD1a), and MB3.6 (anti-GD3). Bovine brain standard gangliosides were applied 1, 3, 5, 7, and/or 9 nmol/lane. Upper left: staining of GM1a by GMB16. GM1b isolated from YAC-1 did not stain with GMB16. Upper right: staining of GD1a by GMR17. GM1b isolated from YAC-1 also stained with GMR17. Lower panel: staining of GM3 and GD3 with resorcinol–HCl (left), and staining of GD3 but not GM3 with MB3.6. GMR17 failed to stain GM3 and GD3, and stained standard GD1a.

neuraminidase from *Macrobdella decora* (CalBiochem, Cat #480706, lot #B52582) suspended in sodium acetate buffer (pH 5.5) for 24 h at 37 °C. The control extracts were treated only with sodium acetate buffer (pH 5.5) for 24 h at 37 °C. The gangliosides were desalted in columns (ENVI-Chrom P, Supelco, Bellefonte, PA). The repurified gangliosides were separated by 2D chromatography as described above. Both experimental and control chromatograms were stained with GMR17, GMB16, and GD1a-1.

Base treatment of gangliosides. *O*-Acetyl groups of gangliosides were removed by base treatment following an earlier procedure [25]. Ganglioside extracts from 50 million cells (HH870 or PC3, two analyses/preparation) were suspended in 100 μl chloroform:methanol (v/v, 1/1) and equal amount of concentrated NH_4OH (14.8 N) was mixed well and incubated for 1 h at room temperature (25 °C). Ammonia was evaporated over N_2.

HPLC purification of gangliosides. Gangliosides purified from PC-3 were applied to a Shimadzu HPLC (Shimadzu, Kyoto, Japan) C-18 column (4.6 mm × 25 cm) and fractionated. Individual gangliosides were then eluted with a programmed gradient of propanol:hexane (55:45) and propanol: water (55:45). The flow rate was adjusted to

0.25 ml/min and 0.5 ml each of the effluent was successively collected. The mono- and disialoganglioside fractions (tubes 25–49) were analyzed by TLC immunostaining.

Immunochemical localization of gangliosides with laser scan confocal microscopy. Live cells were immunostained to examine the distribution of the major gangliosides. For this purpose, CaP and PrEC cells were cultured in sterile 8-well Nunc Lab-Tek II Chamber Slide System (Cat No 154534; Nalge Nunc International, Naperville, IL 60563). For immunochemical observations, 10,000 PrEC or CaP cells were suspended in RPMI 1640 (0.5 ml) with glutamine supplemented with 10% fetal calf serum, Hepes buffer, and antibiotics; the cells were incubated at 37 °C in a humidified (95% air/5% CO_2) chamber. After 24 h, the medium was removed and the cells attached to the bottom of the chamber were washed in cold D-MEM/F-12 medium (Invitrogen; Cat No 11039-021) once and incubated in the same cold medium for 30 min. Further experiments were carried on an ice chamber without exposing the cells directly to ice. The cells were blocked with cold PBS (pH 7.2)–human serum albumin (HSA, 2%) for 2 h and rinsed with PBS–HSA (1%). Primary antibody was diluted in cold PBS–HSA (1%) and the concentration of the antibody was adjusted to 2 ng/ml. The cells were incubated on ice with primary antibody for 90 min and then washed in PBS–HSA (1%) for 5 min, thrice. The cells were then incubated for 30 min in rhodamine red-conjugated goat anti-mouse IgM/fluorescein-isothiocyanate FITC conjugated goat anti-mouse IgG (diluted in cold PBS–1% HSA 1:200) (Jackson Immunoresearch; Cat No : 115-295-075; 115-095-071). After washing the cells in the same cold buffer thrice, the slide was removed from the chamber and mounted with 95% glycerol with 5% phosphate buffer. In some preparations, after final wash, the cells were fixed for one minute in 4% paraformaldehyde (cold). The cells were washed with PBS (without HSA) buffer. The glycerol-mounted slides were refrigerated for a day or two and examined with a laser scan confocal fluorescence microscope (LSCFM, LSM 510 Carl Zeiss, Oberkochen, Germany) equipped with a 514λ argon and a 543λ helium–neon laser. The emitted light reflected from the sample and fluorescence was collected by an oil immersion lens and imaged onto a photomultiplier tube after passing through a confocal aperture at an optical filter.

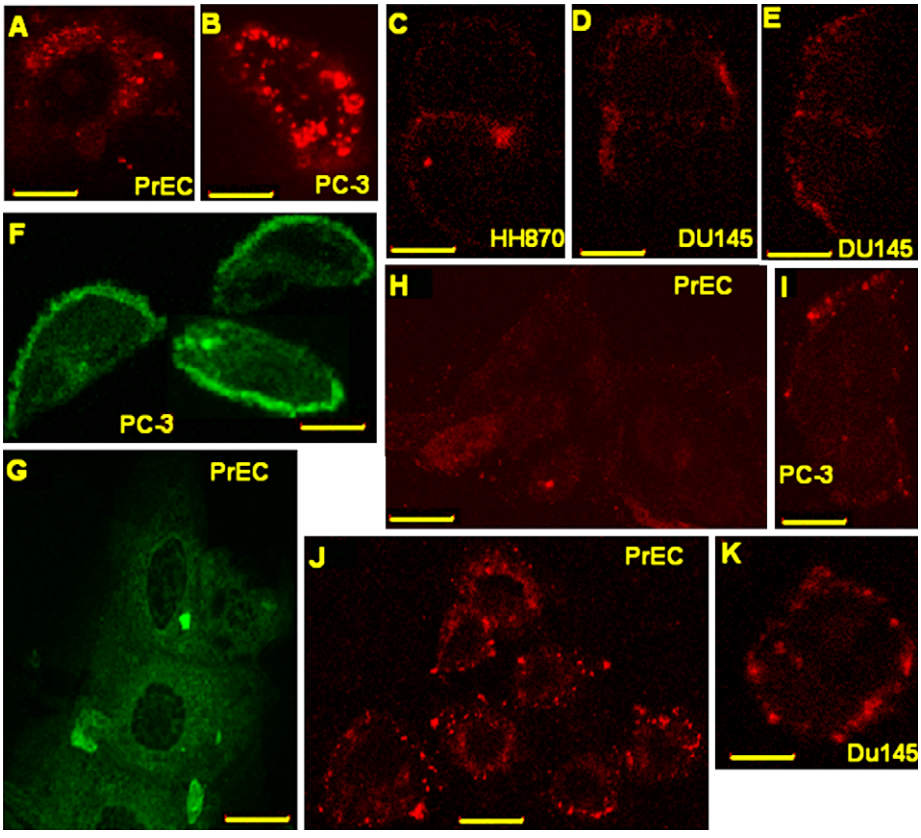

Fig. 2. Confocal fluorescence microscopic assessment of gangliosides in normal prostate epithelial cells (PrEC) and AR (−) prostate cancer cell lines (DU 145, PC-3, and HH870). GMR17 is a monoclonal antibody that reacts to GD1a and GT1b in bovine brain gangliosides and to GD1a, GM1b, and three other unidentified gangliosides in prostate cancer cell lines. (A) GMR17 immunostaining of the cell surface and the cytoplasm of PrEC cells. Ganglioside GD1a but not GM1b is detectable in chromatograms of ganglioside extracts of PrEC. (B) GMR17 stains predominantly the surface of PC-3 cells. Cell-surface clustering of the gangliosides is shown by the bright fluorescent spherules. (C–E) Cell surface distribution of GMR17 positive gangliosides during telophase of HH870 (C), DU 145 (D,E). (F,G) FITC-14.G2a immunostaining. 14.G2a is known to be specific for GD2 but it also stains one or two additional unknown gangliosides in CaP cells. (F) Cell-surface distribution of immunoreactivity of 14.G2a suggests the distribution of GD2 on the cell surface of CaP cells. (G) In contrast, no such cell surface distribution of GD2 (14.G2a immunoreactivity) is observed with normal PrEC. The cytoplasm of normal cells stains weakly. (H) Isotype control for IgM antibodies. Both GMR17 and KM696 are IgM antibodies. Therefore, a non-specific murine IgM was used as isotype control. The isotype control is distinctly negative. (I–K) KM696-rhodamine red staining. KM696 is monospecific for GM2. Cell surface staining for GM2 is observed in PC-3 (I), normal PrEC (J), and DU 145 (K). Vertical line refers to 15 μM (for A, B, F, H, and J) and 10 μM (for C, D, E, G, I, and K). (H–K) These preparations were treated with 4% paraformaldehyde rinse prior to glycerol mounting.

Results

Specificity of monoclonal antibodies in ELISA and TLC

Fig. 1A shows the specificity of eight MAbs. Seven of them were monospecific for their respective gangliosides. GMR17 recognized both GD1a and GT1b in ELISA (Fig. 1A) and in the thin-layer chromatogram (Fig. 1B). GMR17 failed to stain GM1a, GM3, and GD3 (Fig. 1C); however, it stained standard GD1a and GM1b isolated from YAC-1 (murine lymphoma cells) (Fig. 5A). GM1b or GD1a was not recognized by GMB16, a MAb specific for GM1a (Fig. 1C, upper, left). MB3.6 recognized GD3 but not GM3 in the same chromatograms at any concentration (Fig. 1C, lower, middle).

Immunostaining of cell surface ganglioside with monoclonal antibodies: assessment with LSFM

The monoclonal antibodies to GM1a (GMB16), GD1b (GGR12), GT1b (GMR5), and GD3 (MB3.6) did not stain PrEC or CaP cells. The results obtained with other MAbs are presented in Fig. 2. GMR17 stained the cell surface and the cytoplasm of PrEC cells (Fig. 2A) and predominantly the surface of PC-3 cells (Fig. 2B). In addition to uniform staining, distinct fluorescent spherules on the cell surface indicated clustering of the gangliosides during immunostaining. Cell surface distribution of GMR17-positive gangliosides during telophase of HH870 cells (Fig. 2C), DU 145 cells (Figs. 2D and E) showed uniform distribution of GD1a on the cell surface during telophase. MAb 14.G2a, specific for GD2, stained intensely the cell surface of CaP cells (Fig. 2F). In contrast, no such cell surface distribution of GD2 (14.G2a immunoreactivity) is observed with normal PrEC cells (Fig. 2G). The cytoplasm of normal cells stained weakly. The surface and cytoplasm of PrEC and CaP cells were stained by anti-GM2 monoclonal antibody KM696. There is not much difference in the distribution of GM2 between normal and CaP cells, although the gangliosides appeared as distinct clusters on the cell surface (Figs. 2I–K). Both GMR17 and KM696 are IgM antibodies. IgM and IgG isotype controls did not stain the cells (Fig. 2H).

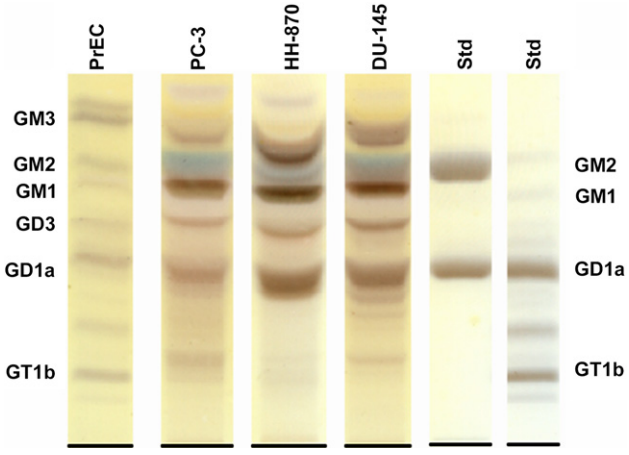

Fig. 3. Ganglioside profiles in normal prostate epithelial cells (PrEC) and AR (−) CaP cell lines stained by resorcinol–HCl in 1D-chromatograms. Each lane contains a ganglioside extract from 25 million cells. The concentration of each ganglioside in the bovine brain standard is 3 nm. (Left to right) PrEC, PC-3, HH870, DU 145, and purified bovine brain GM2, and GD1a, purified bovine brain gangliosides (mixture). The bottom line is the point of application. Solvent system: Chloroform/methanol/0.2% $CaCl_2$ (v/v/v: 55/45/10).

Fig. 4. Ganglioside signatures of AR-negative CaP cell lines in 2D-chromatograms. Each chromatogram contains ganglioside extract obtained from 25 million cells. In the standards (bovine brain gangliosides), the concentration of each ganglioside is 3 nm. (A) Resorcinol–HCl staining of gangliosides from HH870 in the 2D-chromatogram. Vertical line represents direction of flow of the first solvent system, chloroform/methanol/0.2% $CaCl_2$ (55/45/10, v/v/v). Horizontal line represents the direction of flow of the second solvent system, chloroform/methanol/2.5 M ammonia in 0.25% KCl (50/40/10, v/v/v). Note the presence and position of GM3, GM2, GM1, GD1a, and GD2. GM3, GM2, and GD1a appear to be the most prevalent gangliosides. (B) Immunochemical identification of GM2 with KM696 MAb. The solvent systems used for first and second runs were the same as in Fig. 2A. Interestingly, there were two variants of GM2. Right larger spot (1) and Left smaller spot (2). (C) Resorcinol–HCl staining of gangliosides from bovine brain. The conditions were the same as in A. (D) DU 145, PC-3, and HH870 were stained with 14.G2a MAb, which is known to be specific for GD2; however the 2D-chromatogram of PC-3 and HH870 showed two and three distinct spots, respectively. A1 and A2 are unidentified spots that stain with 14.G2a. In HH870 the spot B may represent long chain gangliosides which may include O-AcGT1a, since it did not stain with GMR11 (anti-GT1a IgM antibody), or GQ1b since the mobility lower than GT1b or GT2. (E) 14.G2a-reactivity after NH_4OH-treatment of ganglioside extract from HH870. Spots A1 and A2 have disappeared, indicating that it could be O-AcGD2. Spot B also disappeared, suggesting that it could be O-acetylated GT1a. After base-treatment, GD2-doublets show faster mobility. (F) Immunostaining of HH870 with MB3.6 MAb against GD3. Clearly HH870 expresses GD3. GD3 appears as a doublet due to differences in the length of fatty acids of the ganglioside. (G) Immunostaining of HH870 with anti-GD1a MAb. Two spots were identified. The more intense spot corresponded to GD1a. The upper weak spot corresponded to the position of GM1b.

Fig. 5. Pattern of immunostaining of gangliosides derived from AR (+) CaP cells with GMR17 and 14.G2a. (A) 1D-chromatograms of gangliosides from AR (−) (PC-3, DU 145, and HH870), AR (+) (LNCaP FGC, LNCaP FGC-10), and murine YAC-1 cells immunostained with GMR17 MAb. GM1b, characteristic of YAC-1 cells stained with GMR17. GMR17 stained feebly the AR (+) cells, however GD1a is visible. (B) 1D-chromatogram of gangliosides from normal prostatic epithelium (PrEC). GD1a is not detectable with GMR17. (C) 2D-chromatogram of gangliosides from AR (+) LNCaP FGC cells shows one distinct spot and a weak upper spot. (D) Immunostaining of 1D-chromatograms of AR (−) cells with GGR12 (anti-GD1b). GD1b was not detectable in any of the cell lines tested. (E) GMR5 (anti-GT1b) showing the absence of GD1b and GT1b at detectable level in CaP cells but their strong presence in standards.

Identification of gangliosides in normal and neoplastic prostate epithelial cells by resorcinol–HCl

We used ganglioside extracts from 25 million cells per lane in one-dimensional (1D) or two-dimensional (2D) chromatograms. Commercial bovine brain gangliosides (3 nmol/lane) were used for comparison. The staining intensity of the gangliosides was low in normal cells (PrEC) compared to CaP cells (Fig. 3).

The resorcinol staining intensity and the mobility of standard gangliosides in 1D-chromatograms tentatively identified the gangliosides in the following order, in PrEC cells (Fig. 3): GM3 > GD1a = GT1b > GM2 = GD3 = GD1b > GM1. Gangliosides in PC-3, DU 145,

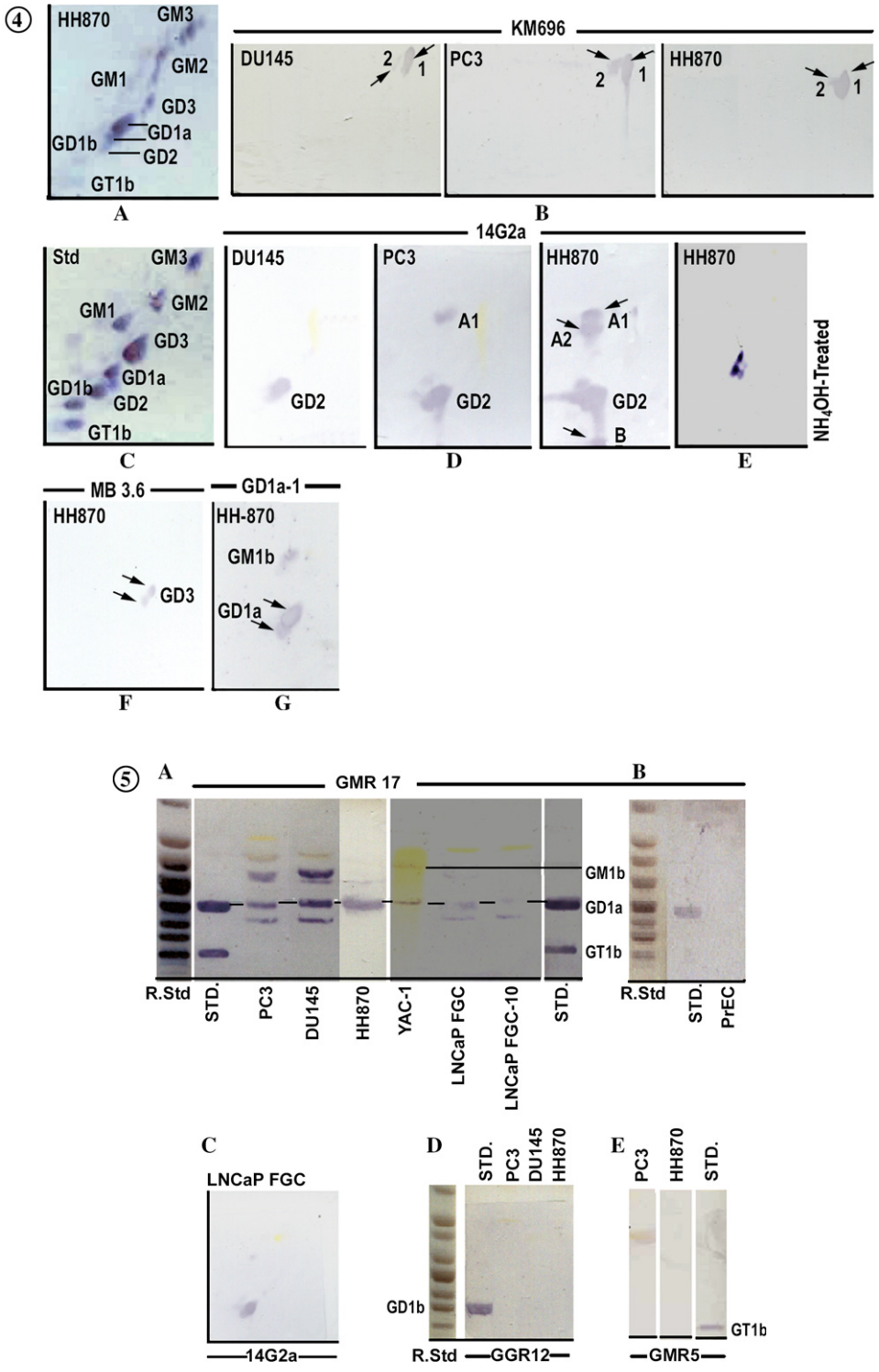

and HH870 cells were: GD1a > GM3 > GM2 > GM1 > GD2 > GD3 > GT1b (GD1b not identified). Resorcinol staining intensity and mobility of the gangliosides from normal and CaP cells in 2D-chromatograms were compared with those of bovine gangliosides. GD1a was the most prevalent ganglioside in all CaP cell lines. Further, these cell lines expressed abundant quantities of GM1, GM2, and GM3 and the presence of GD3 and GD2.

Several gangliosides appeared as doublets, which signify the differences in length, number of double-bonds, and hydroxylation of fatty acid chains and alterations in the sialic acids [10]. Human tissues usually contain *N*-acetyl neuraminic acid (NeuAc) but may contain *N*-glycolyl neuraminic acid (NeuGc), *O*-acetyl neuraminic acid (*O*-Ac NeuAc) or neuraminyl lactone [10], and the last two are susceptible to base treatment [25]. Fig. 4A illustrates three distinct resorcinol-stained spots for GM3 in HH870 cells, whereas in standard (bovine brain gangliosides) only one spot was observed (Fig. 4C). The different spots of GM3 in HH870 could be due to differences in the fatty acids or sialic acids.

Identification of gangliosides by immunostaining

Since none of the murine MAbs for GM3 were specific for GM3, no immunostaining was done to verify the presence of GM3. Moreover, GM3 is common in all extraneural tissues and in both normal and malignant prostate cells.

Murine MAb KM696, specific for GM2, reacted with two distinct spots in the 2D-chromatograms of the ganglioside extracts of PC-3, DU 145, and HH870 (Fig. 4B). The doublets of GM2 reflect differences in the nature of fatty acids (length, presence of double bonds, or hydroxyl groups).

Murine IgG MAb 14.G2a reported to be specific for GD2 [26] stained GD2 distinctly in 2D-chromatograms of all the cell lines (Fig. 4D). While 14.G2a stained only one spot in DU 145 (which is GD2), it reacted with two spots in PC-3 (A1 and GD2 in Fig. 4D) and three spots in HH870 (A1/A2, GD2, and B in Fig. 4D). The mobility of spot A is faster than the main GD2 spot. Such faster mobility could be due to O-acetylation of gangliosides as reported earlier [25]. Spot B was not stained by anti-GT1a IgM (GMR11). It is possible that this spot could be GT2 that reacts often with antibodies to GD2 as in neuroblastoma tumors (Portoukalian, personal communication). Alkali-treatment of the gangliosides from HH870 abolished spots A1, A2, and B (Figs. 4E), indicating that A1 and A2 could be doublets of *O*-acetylGD2 (O-AcGD2) and B could be *O*-acetyl GT1a and not reactive to GMR11. There was a distinct spot (doublet) that was resistant to alkali-treatment. But it showed a shift in mobility to the position of standard GD1a or GD3 (Fig. 4E). The spot was immunostained with MAb 14.G2a but did not react to monoclonal antibodies to GD1a (GD1a-1) or GD3 (MB 3.6) and therefore it is GD2.

Murine MAb to GD3 (MB3.6) was applied to 1D-chromatograms of all CaP lines. MB3.6 identified GD3 in the extracts of HH870 (as a doublet in Fig. 4F) and DU 145 but not in PC-3 cells.

Murine MAb from Seikagaku clone GD1a-1 reacts with GD1a and GM1b but not with any other gangliosides. This MAb was used to stain the 2D-chromatograms of gangliosides purified from HH870. Based on the immunostaining and relative mobility with standard, GD1a (doublet) is the major ganglioside of HH870 (Fig. 4G). A spot higher than GD1a and comparable to the position of GM1 was observed and required further analysis (vide infra).

Status of GM1a, GD1b, and GT1b in CaP cells

MAb GMR17 is known to react with GD1a and GT1b (Figs. 1C and 5A). However, GMR17 failed to stain any of the gangliosides in PrEC cells, suggesting the absence of the ganglioside GD1a and GT1b in PrEC cells (Fig. 5B). Similarly, MAb 14.G2a failed to react with any of the gangliosides in PrEC cells (data not shown) while it stained a single spot of GD2 in AR-positive LNCaP FGC cells (Fig. 5C). It should be noted that GM1a could not be detected in CaP cells by immunostaining (GMB16) (data not shown). Similarly, murine MAbs to GD1b (GGR12) and GT1b (GMR5) revealed that these gangliosides were not present in detectable quantities in the extracts from all cell lines (Figs. 5D and E).

Evidence for the presence of GM1b in CaP cells

Immunostaining of the 2D-chromatograms confirmed that GM2, GD2, and GD1a were the most prevalent gangliosides in the three CaP lines. Although a ganglioside comparable in mobility to GM1 was present in all the cell lines, GMB16 MAb failed to stain GM1a in any of the cell lines. Therefore, the ganglioside migrating to the position corresponding to GM1 might not be GM1a; instead, it might be GM1b. Since GM1b is a major ganglioside of murine YAC-1 cells, gangliosides were extracted and isolated from this cell line (Fig. 5A). GMR17 MAb, which binds to both GD1a and GT1b, also recognized GM1b in YAC-1 cells as well as in all CaP cell lines (Fig. 5A). The relative mobility of GM1b was slightly lower than GM1a (Fig. 6F).

To further investigate GM1b in CaP cells, the 2D-chromatograms of the gangliosides isolated from all three cell lines were stained in resorcinol–HCl (Figs. 6A and D) and immunostained with GMR17 (Figs. 6B and D). The immunoprofile revealed GMR17-reactive gangliosides in five different positions (five spots). The major spot #1 stained very intensely in HH870

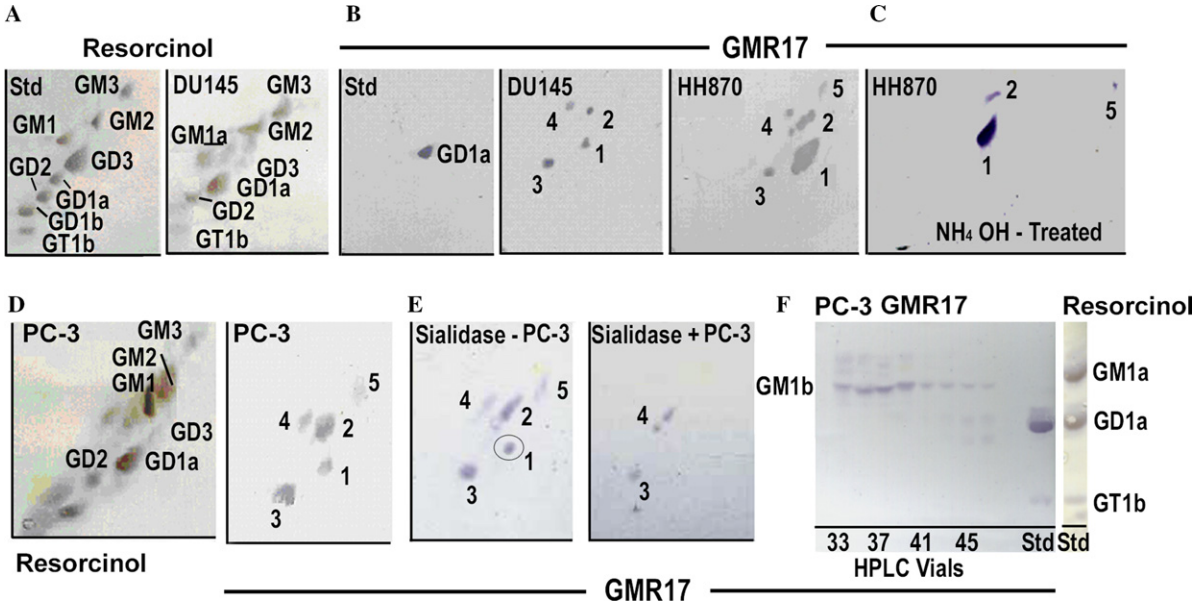

Fig. 6. Immunochemical identification of GD1a, its precursor, and their variants in the ganglioside extracts of CaP cell lines. The solvent systems used for first and second runs are reported in the legend for Fig. 4. Immunostaining of 2D-chromatograms of CaP cell lines was done with GMR17 MAb, which reacts with GD1a and GT1b. GT1b was not detected in any cell line. (A) 2D-chromatogram of standard bovine gangliosides (each ganglioside 3 nmol) and DU 145 stained in resorcinol–HCl. (B) 2D-chromatogram of standard bovine GD1a (3 nmol), DU 145, and HH870 immunostained with GMR17. Four (DU 145) and five (HH870) spots are immunostained with GMR17. Spot #1 is intense in HH870 and corresponds to standard GD1a. Spot #2 was confirmed to be GM1b using gangliosides extracted from murine YAC-1 cell line. (C) GMR17-reactivity after NH_4OH-treatment of ganglioside extract from HH870. Spots #1, #2, and #5 remain, indicating that they are base-resistant. Disappearance of spots #3 and #4 could be due to loss of *O*-acetyl groups or loss of lactone derivatives of the ganglioside GD1a or GM1b. After base-treatment, base-resistant gangliosides showed faster mobility. (D) 2D-chromatogram of PC-3 stained with resorcinol–HCl and with GMR17. Note staining of five spots with GMR17. (E) Sialidase treatment of 2D-chromatogram of PC-3. The sialidase-treated chromatogram was immunostained with GMR17. Spot #1 corresponds to GD1a; Spot #2 corresponds to GM1b; spots #1, #2, and #5 have disappeared, whereas spots #3 and #4 were resistant. The spots that are resistant to the enzyme are O-acetylated gangliosides (C) in which the *O*-acetyl group prevents binding by the enzyme. (F) PC-3 gangliosides were fractionated by HPLC. GM1b and GD1a fractions were stained with GMR 17 to confirm the presence of the gangliosides.

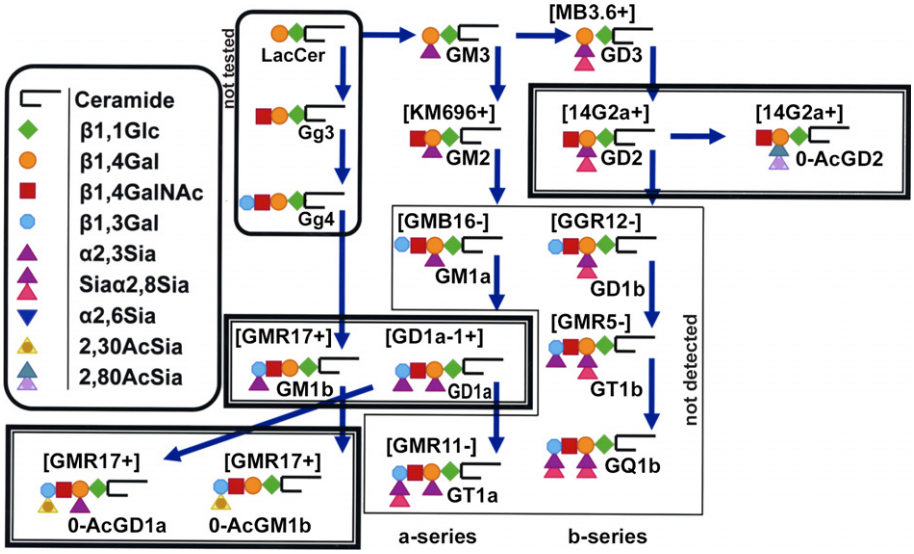

Fig. 7. Two series of ganglioside biosynthetic pathways. GM2, GM1, GD1a, and GT1a belong to ganglioside series called "a-series"; the "b-series" comprises GD3, GD2, GD1b, and GT1b, and GQ1b. The parent of all gangliosides appears to be lactosylceramide (LacCer). In addition to the two series, LacCer gives rise to two neutral lipids, gangliosides 3 and 4 (Gg3 and Gg4). Sialylation of the terminal gal of Gg4 results in GM1b or GM1α. GM1b may give rise to GD1c and GD1α. because there is no GM1a. In prostate tissues, though GM1a is not detectable, GD1a might have been derived from GM1a or by simultaneous bisialylation of Gg4. GMR17 is a unique MAb that identifies a class of gangliosides as indicated. GD1a, stained by GD1a-1, is also reactive with GMR17. Among b-series GD1b and GT1b are not detectable in CaP Cells. Three double-lined boxes encompass gangliosides characteristic of CaP cells.

corresponded to standard GD1a (Fig. 6B), whereas in PC-3 and in DU 145, the GMR17 staining was moderate (Fig. 6D). In HH870, the relative mobility of the spot #1 is comparable to that of the standard GD1a (Fig. 6B). Spot #2 occurs as a doublet in HH870 and as a single spot in PC-3 and DU 145. In PC-3, both spots #2 and #3 were more intense than spot #1. In DU 145 all spots appeared somewhat uniform and faint (Fig. 6B). Spot #5 is seen only in HH870 and PC-3 (Figs. 6B and D).

These different spots may share a common or a general epitope involving sialic acid. In order to understand the nature of gangliosides, we have treated the gangliosides purified from PC-3 and HH870 with α2,3-sialidase as well as subjected to alkali-treatment and resolved in 2D-chromatograms. The results obtained with PC-3 and HH870 were identical. Presence of O-acetylated gangliosides was assessed by the base-treatment of the sample. The extracts of HH870 were subjected to NH_4OH, chromatographed, and immunostained with GMR17. The immunoprofile after base-treatment revealed (Fig. 6C) that the spots #3 and #4, but not spots #1, #2, and #5, were susceptible to base-treatment indicative of the presence of *O*-acetyl groups, which explains as to why these gangliosides were resistant to sialidase treatment. Fig. 6E represents the profile of GMR17-positive spots in PC-3 after α2,3-sialidase treatment. There is a decrease in the number of spots stained by GMR17 after sialidase treatment; Spots #1, #2, and #5 have disappeared. Spots #3 and #4 were resistant to sialidase treatment. This finding further supports the contention that these spots could be due to O-acetylated gangliosides because the *O*-acetyl groups prevent binding of the sialidase.

Spot #2 corresponds to a position lower to GM1a and could be GM1b (Fig. 5A). GM1b purified from YAC-1 cells was also immunostained with clone GD1a-1 MAb, indicating that it is GM1b. To further confirm the presence of GM1b in ganglioside extracts of these cell lines, we used Shimadzu-HPLC to isolate the GM1b fractions (Vials 33–43) (Fig. 6F). The HPTLC profiles were compared with those obtained from YAC-1 cells (data not shown) to confirm the identity of GM1b. Immunostaining with GMR17 further confirmed that the fractions were indeed GM1b.

The immunostaining with different MAbs, together with the observations made with resorcinol staining intensity and the relative mobility with bovine brain gangliosides, provides evidence for the presence of the prostate gangliosides in the following order: Normal PrEC: GM3 > GM2 ≫ GD3 ≫ GD1a; PC-3, DU 145, and HH870 cells: GM3 > GD2 > GD1a > GM2 > GM1b ≫ GD3. Our observations reveal that GD2, *O*-AcGD2, GD1a, and GM1b are the most prevalent gangliosides of AR (−) CaP cells. GD1a and GM1b were present in low concentrations in extracts from AR (+) LNCaP FGC and LNCaP FGC-10 cells (Fig. 5A). However, these cells expressed high levels of GD2 (Fig. 5C) but no additional 14.G2a-reactive spots, including *O*-AcGD2, were observed.

Discussion

Current treatments for AR (−) CaP have not significantly improved survival [27]. Hormonal ablation, the basis of systemic therapy, usually fails to stop eventual progression of metastatic disease [28]. Novel treatment strategies that target-specific signaling pathways, apoptosis, differentiation, or membrane components represent promising alternatives [28]. Tumor-associated gangliosides are membrane antigens that have been successfully used for active immunotherapy of melanoma and colon cancer [29]. Their successful application for active immunotherapy of CaP requires a better understanding of the ganglioside profile of AR (−) CaP cells, particularly the profiles of organ-confined versus metastatic CaP.

Although several AR (−) cell lines from metastatic tumors or viral-transformed prostate epithelial cells (RWPE-1, RWPE-2, and 22Rv-1) are commercially available, development of a cell line from AR (−), organ-confined CaP is difficult because little tissue is available after histopathology. The HH870 CaP cell line is remarkable because it is AR (−) and was developed from a stage T2b organ-confined tumor [19].

Our findings revealed a unique pattern for the ganglioside profile of AR (−) CaP cells. The presence of GM3 is not surprising because it is the most common ganglioside of extraneural tissues [13]. Previous investigators have observed GM3 in normal and neoplastic prostate tissues [16,17]. Our results confirm the reports of Livingston's team [18] on the presence of GM2 in normal and neoplastic prostatic epithelial cells. Results of LSCFM as well as TLC immunostaining with KM696 confirm the presence of GM2 both in normal and neoplastic prostate epithelial cells. Zhang et al. [18] have immunostained frozen sections of normal prostatic epithelial cells and CaP cells with KM696 and reported that both types of tissue stained in equal intensity (4+). Our LSCFM observations confirm their findings on PrEC and CaP cell lines. Since GM2 is expressed in equal density in both normal and neoplastic prostatic epithelial cells, we may infer that GM2 may not be a useful target for antibody-mediated passive or active-specific immunotherapy of CaP. However, TLC-immunostaining with KM696 documents that the intensity of GM2 in PrEC cells is too low compared to that found in CaP cell lines. It is not clear whether tissue culture conditions induce overexpression of GM2 specifically in CaP cells, as reported earlier in melanoma cells grown in vitro [35]. 2D-chromatograms revealed doublets of GM2 in CaP cells (1 and 2 in Fig. 4B), which is due to differences in the nature of the fatty acids

[10,30]. Such a difference is not noticed in normal PrEC cells. While the length and nature of fatty acids in a ganglioside are critical for expression of epitope on the cell surface [10], their length may also alter their exposure to targeting antibodies and the rate of shedding in tumor microenvironment [30]. GD3 was less common in HH870, PC-3, and DU 145 cells. It also occurred as a doublet, which could represent differences in the nature of its fatty acids [30]. GD3 might be the precursor of GD2, the most prominent ganglioside in all three CaP lines.

The 14.G2a MAb is specific for the GD2 epitope [25] and has been employed in passive immunotherapy [31,32]. In our study, 14.G2a was a valuable tool to distinguish differentiation among CaP cell lines. The most striking difference between organ-confined cells (HH870) and bone (PC-3) or brain (DU 145) metastatic CaP was in the number and nature of 14.G2a-reactive fractions. In DU 145 cells, 14.G2a stained a single spot of GD2; in PC-3 and HH870 cells, 14.G2a stained a fraction above GD2. In PC-3, the upper fraction is a single spot (A1), whereas in HH870 cells, the upper fraction is a distinct doublet (A1 and A2). The doublet of upper 14.G2a positive fraction distinguishes HH870 from PC-3. The singlet (A1) in PC-3 and the doublet (A1 and A2) that were susceptible to base-treatment therefore could be *O*-AcGD2. We documented previously that the base-treatment de-*O*-acetylates and reverts O-acetylated gangliosides into the non-*O*-acetyl gangliosides [25]. HH870 also differed from PC-3 in the presence of a slow-moving, intensely staining 14.G2a-reacting fraction below GD2 and closer to the standard GT1b; this fraction did not immunostain with anti-GT1a MAb. Sometimes, extraction procedure may lactonize gangliosides. Lactonized gangliosides differ in their mobility identical to *O*-acetyl gangliosides and are susceptible to base-treatment. If such an artifact were to occur, it will be observed in all cell lines since all of them were treated alike. But, we found the number of spots varied among cell lines. Spot A occurs as a single band in PC–3 and as a doublet in other cell lines. Therefore, we infer that the alkali-susceptibility is not be due to lactone formation but is due to O-acetylated GD2. Similarly, the susceptibility of spot B to base-treatment suggested that it could be an O-acetylated and not a lactonized ganglioside. Diffused and feeble distribution of GD2 in the cytoplasm of PrEC cells and prominent staining and restricted distribution of 14.G2a reactivity on the cell surface of CaP cells suggest that GD2 and *O*-AcGD2 are tumor cell surface-associated gangliosides and could be a potential target for both antibody-mediated passive and active-specific immunotherapy. Because overexpression of GD2 is attributed to cancers with high metastatic potential [33,34], strong expression of GD2 and expression of *O*-AcGD2 and another 14.G2a-positive fraction (Spot B) suggest that organ-confined HH870 cells could be a well-differentiated tumor type with potential invasive characteristic.

The most interesting aspect of the ganglioside signature of AR (−) CaP cell lines was their reactivity to GMR17. MAb GMR17 stained both GD1a and GT1b of the mixture of bovine brain gangliosides (Figs. 1A and 5A), GM1b in YAC-1 cells (Fig. 5A), and five different spots (Figs. 6B and D) in HH870 and PC-3 cell lines, but nothing in PrEC cells (Fig. 5B). In 2D-chromatograms, we observed that one of the GMR17 positive spots (#1) was GD1a. Spot #2 corresponded with GM1b of YAC-1 cells. These observations point out that the gangliosides GD1a and GM1b are indeed CaP-associated antigens. Their distribution on the cell surface was confirmed by LSCFM observations using GMR17 (Figs. 2C–E). Therefore, both GD1a and GM1b could be potential targets for immune recognition. None of the CaP cell lines reacted to GMR5 (anti-GT1b) (Fig. 5E), confirming that GMR17-positivity is not due to GT1b (see Fig. 7).

Expression of some of the gangliosides might be an in vitro artifact of tissue culture conditions. In an earlier study on melanoma-associated gangliosides, expression of GM2 and GD2 could have been due to overexpression of GM2 synthase in tissue culture [35]. High GM2 content in cultured cells may not reflect the native composition of the CaP gangliosides. The same logic cannot be applied to GD2 or GD1a because expression of these gangliosides differed markedly between organ-confined and metastatic cell lines and between AR (+) and AR (−) cell lines, although these cell lines were cultured under identical conditions.

We conclude that CaP cells express GM3, GD3, GM2, GD2, GD1a, and GM1b (Fig. 7). The gangliosides GM1a, GD1b, and GT1b were undetectable (Fig. 7). Unlike AR (+) CaP cells, AR (−) CaP cells strongly express GD1a and GM1b and may express O-acetylated versions of these gangliosides. LSCFM observations on immunostaining of gangliosides confirmed the distribution of the major CaP-associated gangliosides on the cell surface. Therefore, GD2, *O*-AcGD2, GD1a, and GM1b could be ideal targets for passive and active-specific immunotherapy of CaP. Since GM2 expression is high and identical in both PrEC and CaP cells grown in vitro and in vivo ([18] reports 4+ intensity on normal PrEC), it may not be an ideal target for immunotherapy of prostate cancer, unless variants of GM2 (O-acetylation, *N*-glycolyl groups, differences in the length of the fatty acid) are identified in CaP cells. It is in this context, absence of GD2 and GD1a in detectable quantities in normal prostatic epithelial cells, and high and varied (O-acetylated) expression of these two gangliosides make them potential targets for passive and active-specific immunotherapy of CaP.

HH870 overexpressed GD1a, expressed doublets of several gangliosides including GD3, and has three

different gangliosides reactive to 14.G2a (GD2, *O*-AcGD2, and unindentified alkali-labile ganglioside) and two alkali-susceptible and three alkali-resistant gangliosides reactive to GMR17 MAb. Therefore, this cell line may be an ideal component of a polyvalent vaccine for active-specific immunotherapy of CaP, as M10, M24, and M101 cell lines for melanoma [14,29].

Acknowledgments

This investigation is supported by grants from the Department of the United States Army (DAMD17-01-1-0062) and the National Institutes of Health/National Cancer Institute (CA107831-01), and by funding from the Associates of Breast and Prostate Cancer Studies and Santa Monica Research Foundation (Santa Monica, CA). Thanks are due to Ernesto Barron at the EM core facility at Doheny Eye Institute, University of Southern California, for assistance in LSCFM, Thiruverkadu S. Saravanan, Ph.D. and Meena Verma, M.B., B.S., for other technical support.

References

[1] P.M. Gullino, Prostaglandins and gangliosides of tumor microenvironment: their role in angiogenesis, Acta Oncol. 34 (1995) 439–441.
[2] A. Merzak, S. Koochekpour, S. McCrea, Y. Roxanis, C.J. Pilkington, Gangliosides modulate proliferation, migration, and invasiveness of human brain tumor cells in vitro, Mol. Chem. Neuropathol. 24 (1995) 121–135.
[3] G. Alessandri, P. Cornaglia-Ferraris, P.M. Gullino, Angiogenic and angiostatic microenvironment in tumors—role of gangliosides, Acta Oncol. 36 (1997) 383–387.
[4] S. Koochekpour, G.J. Pilkington, Vascular and perivascular GD3 expression in human glioma, Cancer Lett. 104 (1996) 97–102.
[5] K.M. Hedberg, B. Bellheden, C.J. Wikstrand, P. Freedman, Monoclonal anti-GD3 antibodies selectively inhibit the proliferation of human malignant glioma cells in vitro, Glycoconj. J. 17 (2000) 717–726.
[6] S. Yoshida, S. Fukumoto, H. Kawaguchi, S. Sato, R. Ueda, K. Furukawa, Ganglioside G(D2) in small cell lung cancer cell lines: enhancement of proliferation and mediation of apoptosis, Cancer Res. 61 (2001) 4244–4252.
[7] Z. Lang, M. Guerrera, R. Li, S. Ladisch, Ganglioside GD1a enhances VEGF-induced endothelial cell proliferation and migration, Biochem. Biophys. Res. Commun. 282 (2001) 1031–1036.
[8] S. Birkl, G. Zeng, L. Gao, R.K. Yu, J. Aubry, Role of tumor-associated gangliosides in cancer progression, Biochimie 85 (2003) 455–463.
[9] L.D. Bergelson, Serum gangliosides as endogenous immunomodulators, Immunol. Today 46 (1995) 483–486.
[10] H. Wiegandt, Gangliosides, in: H. Wiegandt (Ed.), Glycolipids, Elsevier, Amsterdam, 1985, pp. 199–260.
[11] M.L. Freimer, K. McIntosh, R.A. Adams, C.R. Alving, D.B. Drachman, Gangliosides elicit a T-cell independent antibody response, J. Autoimmun. 6 (1993) 281–289.
[12] R.F. Irie, D.L. Morton, Regression of cutaneous metastatic melanoma by intralesional injection with human monoclonal antibody to ganglioside GD2, Proc. Natl. Acad. Sci. USA 83 (1986) 8694–8698.
[13] P.O. Livingston, Approaches to augmenting the immunogenicity of melanoma gangliosides: from whole melanoma cells to ganglioside–KLH conjugate vaccines, Immunol. Rev. 145 (1995) 147–166.
[14] M.H. Ravindranath, D.L. Morton, Role of gangliosides in active immunotherapy with melanoma vaccine, Int. Rev. Immunol. 7 (1991) 303–329.
[15] M.H. Ravindranath, D.L. Morton, Immunogenicity of membrane-bound gangliosides in viable whole-cell vaccines, Cancer Invest. 15 (1997) 491–499.
[16] T. Shiraishi, M.T. Kinter, S.E. Mills, M.C. Lippert, G.S. Bova, W.W. Young Jr., The glycosphingolipids of human prostate tissue, Biochim. Biophys. Acta 961 (1988) 164–169.
[17] M. Satoh, Y. Fukushi, S. Kawamura, C. Ohyama, S. Saito, S. Orikasa, E. Nudleman, S. Hakamori, Glycolipid expression in prostatic tissue and analysis of the antigen recognized by antiprostatic monoclonal antibody APG1, Urol. Int. 48 (1992) 20–24.
[18] S. Zhang, H.S. Zhang, V.E. Reuter, S.F. Slovin, H.I. Scher, P.O. Livingston, Expression of potential target antigens for immunotherapy on primary and metastatic prostate cancers, Clin. Cancer Res. 4 (1998) 295–302.
[19] S.R. Selvan, A.N. Cornforth, N.P. Rao, Y.A. Reid, P.M. Schiltz, R.P. Liao, D.T. Price, S.F. Heinemann, R.O. Dillman, Establishment and Characterization of a Human Primary Prostate Carcinoma Cell Line, HH870. Prostate (2004), in press.
[20] R.W. Ledeen, R.K. Yu, Gangliosides: structure, isolation and analysis, Methods Enzymol. 83 (1982) 139–141.
[21] I. Popa, C. Vlad, J. Bodennec, J. Portoukalian, Recovery of gangliosides from aqueous solutions on styrene-divinylbenzene copolymer columns, J. Lipid Res. 43 (2002) 1335–1340.
[22] T.C. Comas, T. Tai, D. Kimmel, B.W. Scheithauer, P.C. Burger, D.K. Pearl, S.D. Jewell, A.J. Yates, Immunohistochemical staining for ganglioside GD1b as a diagnostic and prognostic marker for primary human brain tumors, Neuro-oncology 1 (1999) 261–267.
[23] M. Kotani, H. Ozawa, I. Kawashima, S. Ando, T. Tai, Generation of one set of monoclonal antibodies specific for a-pathway ganglioseries gangliosides, Biochim. Biophys. Acta 1117 (1992) 97–103.
[24] M.H. Ravindranath, R.M.H. Ravindranath, D.L. Morton, M.C. Graves, Factors affecting the fine specificity and sensitivity of serum antiganglioside antibodies in ELISA, J. Immunol. Methods 169 (1994) 257–272.
[25] M.H. Ravindranath, J.C. Paulson, R. Irie, Human melanoma antigen O-acetylated ganglioside (GD3) is recognized by Cancer antennarius lectin, J. Biol. Chem. 263 (1988) 2079–2086.
[26] K. Mujoo, T.J. Kipps, H.M. Yang, D.A. Cheresh, U. Wargalla, D.J. Sander, R.A. Reisfeld, Functional properties and effect on growth suppression of human neuroblastoma tumors by isotype switch variants of monoclonal antiganglioside GD2 antibody 14.18, Cancer Res. 49 (1989) 2857–2861.
[27] V.J. Assikic, J.W. Simons, Novel therapeutic strategies for androgen-independent prostate cancer: an update, Semin. Oncol. 31 (2004) 26–32.
[28] J. Gulley, W. Dahut, Novel clinical trials in androgen-independent prostate cancer, Clin. Prostate Cancer 1 (2002) 51–57.
[29] D.L. Morton, E.C. Hsueh, R. Essner, L.J. Foshag, S.J. O'Day, A. Bilchik, R.K. Gupta, D.S. Hoon, M. Ravindranath, J.A. Nizze, G. Gammon, L.A. Wanek, H.J. Wang, R.M. Elashoff, Prolonged survival of patients receiving active immunotherapy with Canvaxin therapeutic polyvalent vaccine after complete resection of melanoma metastatic to regional lymph nodes, Ann. Surg. 236 (2002) 438–449.
[30] E. Nudelman, S. Hakomori, R. Kannagi, S. Levery, M.Y. Yeh, K.E. Hellstrom, I. Hellstrom, Characterization of a human

melanoma-associated ganglioside antigen defined by a monoclonal antibody, 4.2, J. Biol. Chem. 257 (1982) 12752–12756.
[31] M.M. Uttenreuther-Fischer, C.S. Huang, R.A. Reisfeld, A.L. Yu, Pharmacokinetics of anti-ganglioside GD2 mAb 14.G2a in a phase I trial in pediatric cancer patients, Cancer Immunol. Immunother. 41 (1995) 29–36.
[32] R. Handgretinger, P. Baader, R. Dopfer, T. Klingebiel, P. Reuland, J. Treuner, R.A. Reisfeld, D. Niethammer, A phase I study of neuroblastoma with the anti-ganglioside GD2 antibody 14.G2a, Cancer Immunol. Immunother. 35 (1992) 199–204.
[33] D.A. Cheresh, Human melanoma cell attachment involves an Arg-Gly-Asp-directed adhesion receptor and the disialoganglioside GD2, Prog. Clin. Biol. Res. 288 (1989) 3–24.
[34] D.A. Cheresh, M.D. Pierschbacher, M.A. Herzig, K. Mujoo, Disialogangliosides GD2 and GD3 are involved in the attachment of human melanoma and neuroblastoma cells to extracellular matrix proteins, J. Cell Biol. 102 (1986) 688–696.
[35] T. Tsuchida, M.H. Ravindranath, R.E. Saxton, R.F. Irie, Gangliosides of human melanoma: altered expression in vivo and in vitro, Cancer Res. 47 (1987) 1278–1281.